Implementation of Evaluating Bridge Behavior Using Ultra-High-Resolution Next-Generation Digital Image Correlation (DIC): Applications in Bridge Inspection and Damage Assessment, Final Report

Technical Report 5-6950-01-1
Project 5-6950-01
Cooperative Research Program

https://library.ctr.utexas.edu/hostedpdfs/utsa/5-6950-01-1.pdf

UNIVERSITY OF TEXAS AT SAN ANTONIO
DEPARTMENT OF CIVIL AND ENVIRONMENTAL ENGINEERING
SAN ANTONIO, TEXAS 78249

in cooperation with the
Federal Highway Administration and the
Texas Department of Transportation

Technical Report Documentation Page

1. Report No. FHWA/TX-23/5-6950-01-1	2. Government Accession No.	3. Recipient's Catalog No.
4. Title and Subtitle Implementation Evaluating Bridge Behavior Using Ultra-High-Resolution Next-Generation Digital Image Correlation (DIC): Applications in Bridge Inspection and Damage Assessment		5. Report Date Submitted: August 2022 6. Performing Organization Code
7. Author(s) Shima Rajae, PhD; Rasool Ghorbani, PhD; Seyed Sasan Doalti, https://orcid.org/0000-0002-9255-3547; Wassim M. Ghannoum, PhD, https://orcid.org/0000-0003-2631-7690		8. Performing Organization Report No. 5-6950-01-1
9. Performing Organization Name and Address University of Texas at San Antonio Department of Civil and Environmental Engineering One UTSA Circle San Antonio, TX 78249		10. Work Unit No. (TRAIS) 11. Contract or Grant No. 5-6950-01
12. Sponsoring Agency Name and Address Texas Department of Transportation Research and Technology Implementation Division 125 E. 11th Street Austin, TX 78701		13. Type of Report and Period Covered Implementation Report July 2021– August 2022 14. Sponsoring Agency Code
15. Supplementary Notes Project performed in cooperation with the Texas Department of Transportation and the Federal Highway Administration.		
16. Abstract The Civil Infrastructure Vision (CIV) system is an integrated software/hardware system is based on principles of Digital Image Correlation (DIC) developed at UTSA for TxDOT. The system can be used to monitor surface deformations on bridges to accuracies on the order of 1/1,000th in. Project objectives included training TxDOT on using the system during load testing and processing the resulting deformation data. Ten bridges were load tested over a period of one year using CIV. Throughout this project, procedural improvements were made to accelerate load testing and minimize traffic disruptions. In the end, the team was able to complete the full process, from arriving to a site through finishing repacking equipment, in less than two hours. This allowed up to three load tests in one day; a much faster process than using traditional instruments, with which a load test could take several days and require direct access to a bridge underside.		
17. Key Words Bridges, load testing, non-contact measurements, load rating, digital image correlation	18. Distribution Statement No restrictions. This document is available to the public through the National Technical Information Service, Alexandria, Virginia 22312; www.ntis.gov.	

19. Security Classif. (of report)	20. Security Classif. (of this page)	21. No. of pages	22. Price
Unclassified	Unclassified	31	

Form DOT F 1700.7 (8-72) Reproduction of completed page authorized

TxDOT Project 5-6950-01

Final Project Report 5-6950-01-1

Implementation of Evaluating Bridge Behavior Using Ultra-High-Resolution Next-Generation Digital Image Correlation (DIC):

Applications in Bridge Inspection and Damage Assessment, Final Report

The University of Texas at San Antonio

Shima Rajae

Rasool Ghorbani

Seyed Sasan Doalti

Wassim M. Ghannoum

Submitted August 30, 2022

Project Title: Implementation of Evaluating Bridge Behavior Using Ultra High-Resolution Digital Imaging Correlation (DIC)

Sponsoring Agency: Texas Department of Transportation

Performing Agency: The University of Texas at San Antonio

Project performed in cooperation with the Texas Department of Transportation and the Federal Highway Administration.

DISCLAIMER

The contents of this report reflect the views of the authors, who are responsible for the facts and the accuracy of the data presented herein. The contents do not necessarily reflect the official view or policies of the Federal Highway Administration (FHWA) or the Texas Department of Transportation (TxDOT). This report does not constitute a standard, specification, or regulation.

Engineering Disclaimer

NOT INTENDED FOR CONSTRUCTION, BIDDING, OR PERMIT PURPOSES.

Project Engineer: Wassim M. Ghannoum

Professional Engineer License State and Number: Texas No. 121170

P.E. Designation: Research Supervisor

ACKNOWLEDGMENTS

The contributions to load testing and guidance of the following Texas Department of Transportation employees are gratefully acknowledged: Biniam Aregawi, Steven Austin, Graham Bettis, Drake Builta, Bernie Carrasco, Francisco Flores, Leon Flournoy, Seth Franks, Joshua Gutzwiller, Istiaque Hasan, Yi Qiu, Hafiz Rahman, Alex Marjil Rodriguez, Tom Schwerdt, and Mark Wallace.

CONTENTS

1 Introduction 1

1.1 General 1

1.2 Content 1

2 Bridge Load Tests 2

2.1 Overview of Bridges 2

2.2 CIV System Setup 4

2.3 Loading Protocol 4

2.4 Outcomes 6

2.4.1 Efficiency 6

2.4.2 Load rating 6

3 Sample Data Processing 7

3.1 Introduction 7

3.2 Case study 1: Flat slab bridge 7

3.2.1 Bridge description 7

3.2.2 Load testing procedures 8

3.2.3 Load testing results 11

3.3 Case study 2: Multi girder steel bridge 15

3.3.1 Bridge description 15

3.3.2 Load testing procedures 16

3.3.3 Load testing results 18

3.3.4 Experimental LLDFs 20

3.4 Summary and Conclusions 22

4 Value of Research 23

5 References 25

LIST OF TABLES

Table 2-1: Tested Bridges 2
Table 3-2: Calculations of experimental DFM for each strip under fixed-location loading with tandem axels at midspan and for single-lane loading and projected two-lane loading 14
Table 3-3: Measured test deflections and corresponding girder LLDFs 20

LIST OF FIGURES

Figure 2-1: Images of the 10 load-tested bridges 3
Figure 2-2: Two loading trucks on Bridge 05 5
Figure 3-1: Photograph of flat slab concrete bridge 8
Figure 3-2: Attachment of HCPTs at midspan on the bridge slab soffit. 9
Figure 3-3: selection of targets and user-defined coordinate system 9
Figure 3-4: Bridge cross-section geometry and truck path 10
Figure 3-5:Truck properties 10
Figure 3-6: Deflection histories of midspan targets during the crawl-speed test 11
Figure 3-7: Vertical deflection histories of midspan targets during fixed-location test 2 (under tandem axle) 12
Figure 3-8: Deflection of the target across width of the bridge at midspan under fixed-location test 2 12
Figure 3-9: Assumed deflections across bridge cross-section under two trucks with tandem axel position over midspan 13
Figure 3-10: Comparison of estimated equivalent widths for each strip with AASHTO methods. 15
Figure 3-11: image of bridge 16
Figure 3-12: bridge suspended span section 16
Figure 3-13: attachment of HCPTs to the bridge steel girders. 17
Figure 3-14: HCPTs selected in the CIV system and the defined new coordinate system 17
Figure 3-15: Bridge cross-section and truck path a) single truck path b) double truck path 18
Figure 3-16: Trucks properties. 18
Figure 3-17: Vertical deflection histories of midspan targets during fixed-location test 2 (under tandem axle) 19
Figure 3-18: Deflection of the steel girders at midspan under fixe-location test 2 20
Figure 3-19: Live Load Distribution Factors for girders using load test deflection measurements, compared to LLDF estimated using AASHTO standard specifications and AASHTO LRFD 22

1 Introduction

1.1 General

The Civil Infrastructure Vision (CIV) system is an integrated software/hardware system that can be used to monitor surface deformations on structural components ranging from small-scale material-test coupons, to full-scale bridge members. *In the Bridge Calibration edition, the CIV system is calibrated for measuring deformations on large-scale specimens that are 40ft to 110ft away from the cameras. The horizontal fields of view corresponding to those offset distances range from 17ft to 47ft*[1]*.* The non-contact system offers several advantages over traditional contact measurement methods, including: ease and speed of setup, reduction of traffic disruptions, and distributed measurements over large areas of a structural system (as opposed to point measurements).

The system is based on principles of Digital Image Correlation (DIC) and spatial triangulation to determine the 3D spatial coordinates of user-selected targets. In the CIV system, targets can be selected at any point on the surface of the structural system being monitored.

A CIV system was delivered to TxDOT following research project 0-6950, and this implementation project (5-6950-01) was geared towards training TxDOT personnel on using the system and processing the data that originates from it. In all 10 bridge load tests were conducted. Bridge deformations were monitored using the CIV system.

1.2 Content

This report summarizes the location and type of bridges that were load tested as part of this project (Chapter 2). Sample data processing for two bridges are presented in Chapter 3. Value of Research for the project is presented in Chapter 3.

2 Bridge Load Tests

2.1 Overview of Bridges

In all 10 bridges were load tested over a period of one year. The bridges showed inadequate load rating when evaluated using the AASHTO LFR procedures, typically for specialized hauling vehicles or emergency vehicles. However the bridges that were considered had capacities within 10% of those required, indicating that load testing may be beneficial in removing load restrictions for those bridges. All bridges were in relatively good condition and did not exhibit damage or deterioration that would indicate reduced capacities. All bridges carried two lanes of traffic; in some bridges traffic lanes were for opposite direction traffic, and in other for traffic in the same direction. Bridge information is summarized in Table 2-1. Pictures of the bridges that were tested are shown in Figure 2-1.

Table 2-1: Tested Bridges

Bridge Number	Test Date	Road Designation	Bridge Superstructure Type – tested span	Tested Span (ft)
01	2021-06-17	FM1957	Concrete flat slab – simply supported between caps	29
02	2021-08-25	US48	Multi-span steel girder – simply supported span supported by overhangs	52
03	2021-09-16	SH81	Concrete box culvert – continuous span	10
04	2022-02-10	US70	Concrete box culvert – simply supported span	8
05	2022-05-03	SH16	Simply support steel girder – simply supported between caps	22
06	2022-05-03	SH29	Simply support concrete prestressed – simply supported between caps	40
07	2022-05-12	FM2114	Simply support steel girder – simply supported between caps	29
08	2022-05-12	FM2114	Simply support steel girder – simply supported between caps	29
09	2022-05-12	FM2114	Simply support steel girder – simply supported between caps	29
10	2022-05-19	US90	Simply support steel and concrete prestressed girders – continuous spans	52

Figure 2-1: Images of the 10 load-tested bridges

2.2 CIV System Setup

The first task was to identify the best position for the CIV system cameras. Consideration were given to accessibility, line of sight, as well as the desired field of view. When possible closer positioning is preferred as accuracy and noise level in the data improve when the cameras are closer to the bridge. In addition, to further improve noise level in the data, cameras were positioned as level as practical with the bridge with the cameras facing as normal to the bridge sides as possible. This positioning makes the vertical deformations of a bridge occur mostly along the camera sensor planes (with minimal out-of-plane movement), which minimizes noise levels and improves accuracy [1].

Depending on crew size, targets were attached to the underside of bridges, either concurrently or after camera placement. While the CIV system can monitor targets virtually anywhere on the surface of a bridge, attaching targets facilitated target selection at desired locations where deformations readings were needed. Targets were attached by hand when bridge height was low or by extension pole when the bridge was higher. For Bridge 10, a lift was used to attach the targets given the bridge height (Figure 2-1).

2.3 Loading Protocol

A consistent loading protocol was applied to all bridges. Two dump trucks with rear tandem axel load of about 34 to40 kips were used in all cases (Figure 2-2). Trucks were position in three layouts for all bridges. In Layout 1, a single truck was positioned with its front axle at midspan and outer edge of right tires at the edge of the lane closest to the most critical member. Typically edge members were the critical members for load rating. In Layout 2, the same truck was positioned with the rear tandem axels at mid span and right-most tires at the edge of the critical lane. In Layout 3, two trucks are positioned centered within the lane widths with their rear tandem axel at midspan (Figure 2-2).

Prior positioning the trucks and loading the bridges, traffic was stopped for a few minutes to mark the road way for truck locations.

Figure 2-2: Two loading trucks on Bridge 05

Once all preparatory tasks were concluded, load tests proceeded in the following steps:

1- Traffic was stopped
2- The location of targets attached to the underside of bridges was monitored for about 30 seconds to get a zero-load reference
3- The first truck was moved into position for Layout 1
4- Truck engine was stopped to minimize vibrations
5- About 1 minute waiting period was observed to allow for bridge vibrations to settle from truck movement (this step was most critical for longer span bridges that could see measurable bounce from truck movement)
6- The location of targets attached to the underside of bridges was monitored for about 30 seconds
7- The truck was moved off the bridge
8- The location of targets attached to the underside of bridges was monitored for about 30 seconds to get an updated zero-load reference
9- The first truck was moved into position for Layout 2
10- Steps 4 through 8 were repeated
11- Both trucks were moved on the bridge for Layout 3
12- Steps 4 through 8 were repeated
13- Traffic was released

All the steps typically took less than 10 minutes to minimize traffic disruptions.

2.4 Outcomes

2.4.1 Efficiency

Throughout the load tests, procedural improvements were made to accelerate load testing and minimize traffic disruptions. In the end, the full process from arriving to a site up to completing equipment packing was able to be done in less than 2 hours, with a crew of four. When a crew of four is available, camera setup, target placement, roadway marking, and coordination with traffic crews could be performed concurrently. Gained efficiencies allowed the project team and TxDOT to conduct three load tests in one day on bridges that were a few miles apart (Bridges 07, 08, 09); without having been on site prior to testing day.

2.4.2 Load rating

While not the focus of this report, data delivered from the CIV system allowed several of the bridges to be alleviated from load posting. Chapter 3 illustrates a couple of examples for how data from the CIV system can be used to improve the accuracy of load rating.

3 Sample Data Processing

3.1 Introduction

In the United States, the load rating methodology of American Association of Highway and Transportation Officials (AASHTO) Manual for Bridge Evaluation MBE[2] is typically used for determining live load capacity of bridges. The TxDOT Bridge Inspection Manual[3] bases load rating procedures on AASHTO MBE, in which the methodology is based on as-built section properties and materials for strength evaluation; while it provides live load distribution factors that help determine the amount of load carried by individual members. In previous studies, load distribution factors have been shown to provide conservative estimates for load sharing, which may trigger unnecessary load posting or other interventions. Load testing of bridges can provide a more accurate representation of load sharing between bridge members, which may result in higher load rating than estimated using standard methodology. However, load testing of bridges using traditional contact instrumentation is expensive, time consuming, and requires access to bridges, which may not be practical or possible.

The Civil Infrastructure Vision (CIV) system developed as part of TxDOT Project 0-6950 has two high-resolution digital cameras and is able to monitor the three-dimensional movement of virtually any point on a bridge surface from distances up to 110 ft from the cameras. Advantages of the system over traditional contact instrumentation include its relative low cost, ease of operation, speed of setup, ability to monitor any point over a large field of view in a single setup, and its relatively high accuracy, which is necessary for assessing structural capacity from deformation measurements. CIV system measurement accuracy and resolution are quantified in[1, 4, 5].

Two case studies are presented where the CIV system is used to estimates in-situ load sharing for one concrete flat slab bridge (Bridge 1) and one multi-girder steel bridge (Bridge 02) during load testing. The aims of this study were: 1) to demonstrate the effectiveness of the CIV system in monitoring bridge deflections during the load testing, 2) to investigate the distribution of live loads in two types of bridges, and 3) to compare the distribution factors for bending resulting from the load tests with distribution factors calculated from AASHTO standard specifications and AASHTO LRFD [6]. Results indicate that load testing for these bridge types can provide improvements in load rating capacities through more accurate live load distribution.

3.2 Case study 1: Flat slab bridge

3.2.1 Bridge description

The bridge considered in this case study is located in central Texas and was built in 1958. It carries two lanes of traffic, one in each direction, with an Annual Average Daily Traffic (AADT)

count of about 4,000. The bridge consists of simply supported reinforced concrete cast-in-place flat slabs resting on full-width bent caps (Figure 3-1). The bridge has eight simply supported spans for a bridge total length of 60.96 m (200ft). The controlling span for load rating has a length of 7.62 m (25ft). The deck type is cast in place concrete, with 35.5 cm (14in.) thickness and 5cm (2in.) of asphalt overlay. The bridge deck was measured to be 9.08m (29.8ft) wide with an approach roadway width of 8.23m (27ft).

Per the National Bridge Inventory (NBI 2016), the bridge deck condition rating is 7 (Good with some minor problems), the superstructure condition rating is 6 (Satisfactory with minor deterioration of structural elements), and the substructure condition rating is 5 (Fair Condition with minor deterioration of structural elements). Based on previous calculation conducted by TxDOT using AASHTO Standard specifications (LFR), the bridge span cannot carry Specialized Hauling Vehicles SU5, SU6, and SU7 and load posting is recommended.

Figure 3-1: Photograph of flat slab concrete bridge

3.2.2 Load testing procedures

Load testing was conducted in June of 2021. The primary objective was to obtain data from which live load distribution across the flat slab could be determined. Deflection data were the primary data collected during testing. Strain data measured on the surface were not used as such data are highly depended on crack locations with respect to the gage length over which stain are measured [7]. While the CIV system can track the movement of any point on a bridge surface, High Contrast Physical Targets (HCPTs) were attached underneath the bridge slab at midspan of the

controlling span and at distance of approximately 1.2m (4ft) apart from each other (Figure 3-2). This placement enabled the team to reliably select tracking targets at the desired midspan locations. In addition, HCPTs provide a high-contrast object (black on white pattern) that minimizes the noise level of the measurement data when tracked by the DIC software.

Figure 3-2: Attachment of HCPTs at midspan on the bridge slab soffit.

The cameras were placed16.45 m (54ft) away from the closest edge of the bridge deck. The resulting field of view is shown in Figure 3-3, which presents a sample image taken from one of the cameras of the CIV system during testing. The CIV system allows users to select a user coordinate system with respect to which target three-dimensional coordinates are provided. The selected targets and user-defined coordinate system are shown in Figure 3-3.

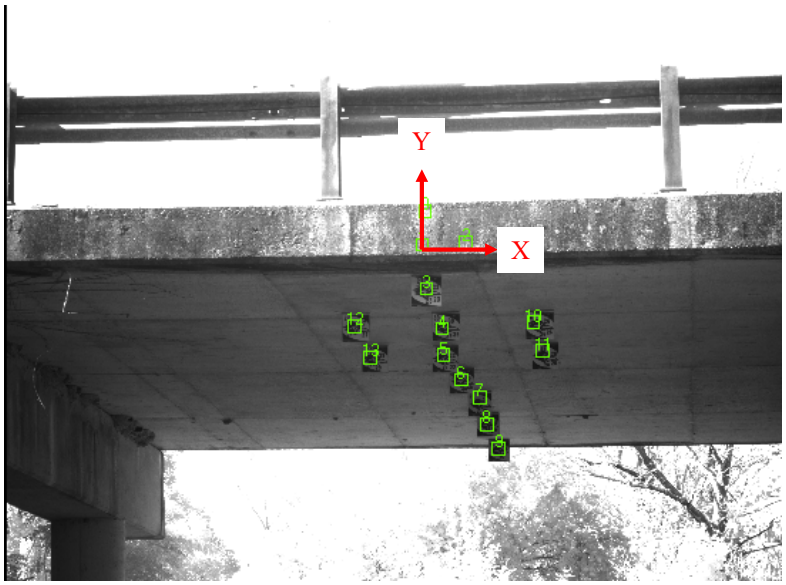

Figure 3-3: selection of targets and user-defined coordinate system

One load testing path was used along which the test truck was placed. The designated truck path placed the centerline of the wheels on one side of the truck at 0.61m (2ft) from the bridge guardrail, per AASHTO MBE [2] (Figure 3-4). This truck positioning is intended to maximize loading on the edge of the bridge slab. Only one truck and one load path were used for load testing, since the bridge is symmetric about its roadway centerline.

The dump truck used for testing had one front single axle and one tandem rear axle, as depicted in Figure 3-5. The front axle of the truck weighed 53.38kN (12,000lbs.), while the tandem axle weighed 177.92 kN (40,000 lbs.).

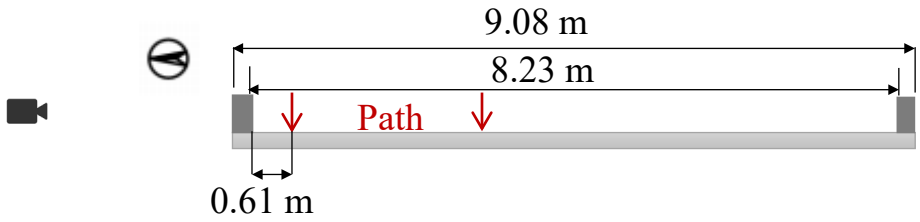

Figure 3-4: Bridge cross-section geometry and truck path

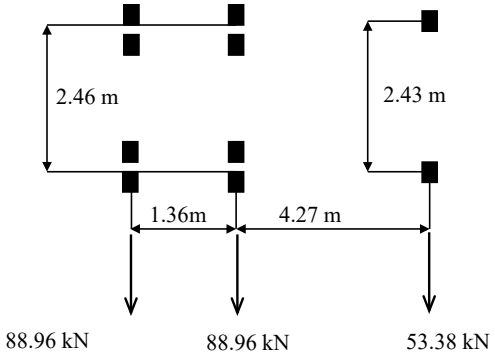

Figure 3-5:Truck properties

The loaded truck was stopped in two positions along the path, during which time deflection data were recorded. In the first position (fixed-location test 1), the front wheels were located at midspan along the path, while for the second position (fixed-location test 2), the rear tandem wheels were placed at midspan. In addition, a crawl-speed test, was conducted during which the truck was driven at a speed less than 8 km/h (<5mph) along the designated path.

Before each test, the three-dimensional location of targets (Figure 3-3) were recorded with no traffic or load on the bridge and used as the baseline location from which deflections were calculated. For each fixed-location test, the truck was stopped for less than a minute at the desired location and the engine cut to minimize bridge vibrations. For the crawl-speed test, the reference state of the bridge was recorded before the proceeded across the bridge at reduced speed while data were recorded. For all reference readings and fixed-location readings, target

locations were recorded for at least 30 image frames and the mean target coordinates were used in deflection calculations. This process reduced the impact of data noise on the measurements. Images were recorded at three frames per second.

3.2.3 Load testing results

3.2.3.1 Deflection measurements

The history of the vertical deflections of select targets at midspan during the crawl-speed test are shown in Figure 3-6. Moving average smoothing with a window size of five frames is applied to the data. As it can be seen in Figure 3-6, targets 3, 5 and 6, located under the truck, sustained a similar deflection history. The maximum deflections for targets 3, 5 and 6 occurred when the tandem axle of the truck crossed over their location. Targets 8 and 9, which are located under the traffic lane that was not loaded, sustained a similar deflection history. Maximum vertical deflections during the crawl-speed test for targets 3,4,5,6,7,8 and 9 were 2.7813 mm (0.1095 in.), 2.7827 mm (0.1131 in.), 2.9058 mm (0.1144 in.) ,2.8956 mm (0.114 in.), 3.1394 mm (0.1236 in.), 3.2766 mm (0.129 in.) and 2.9260 mm (0.1152 in.), respectively.

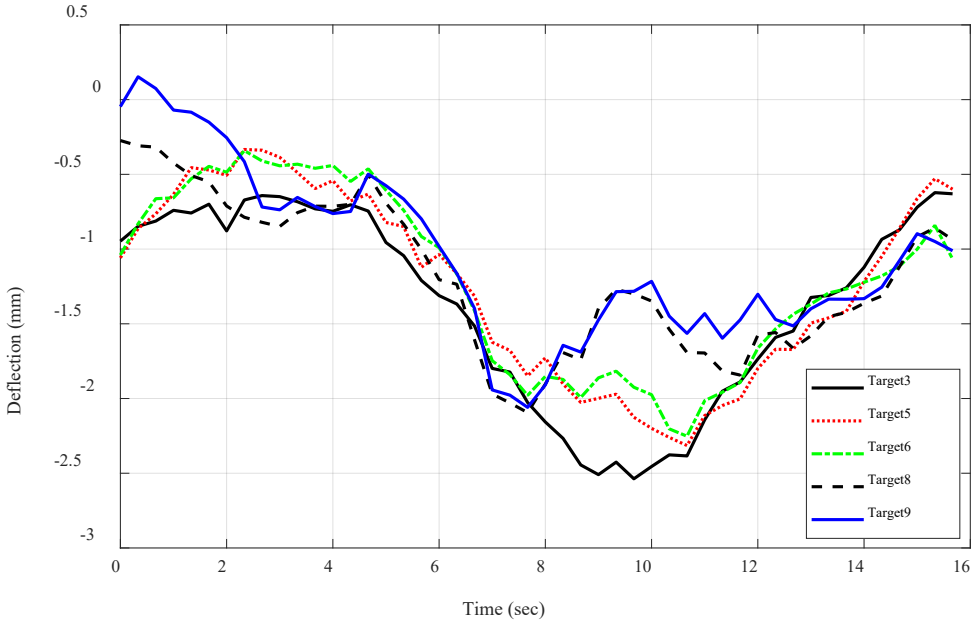

Figure 3-6: Deflection histories of midspan targets during the crawl-speed test

The history of the vertical deflections for fixed-location test 2 are presented in Figure 3-7, while the mean deflections during fixed-location test 2 of the midspan targets are plotted across the cross-section of the bridge in Figure 3-8 Locating the tandem axels at midspan in this test produces the maximum live load moment in the slab. Maximum deflections of the slab during this test occurred at targets 0 and 3, and 6 and 7, which were located approximately under the

truck tandem wheels. Deflections away from the wheel contact points were lower across the midspan cross-section as seen in Figure 3-8.

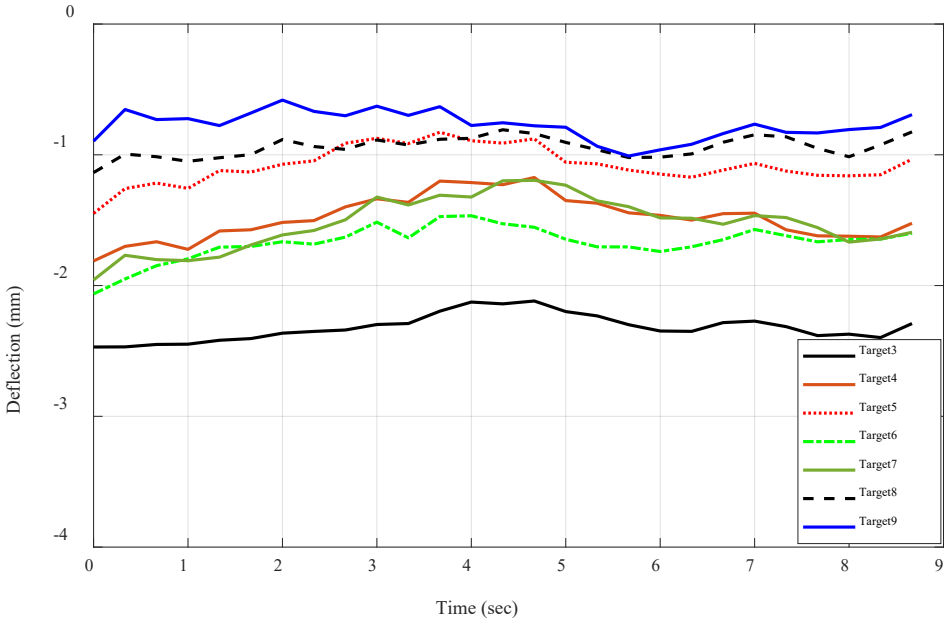

Figure 3-7: Vertical deflection histories of midspan targets during fixed-location test 2 (under tandem axle)

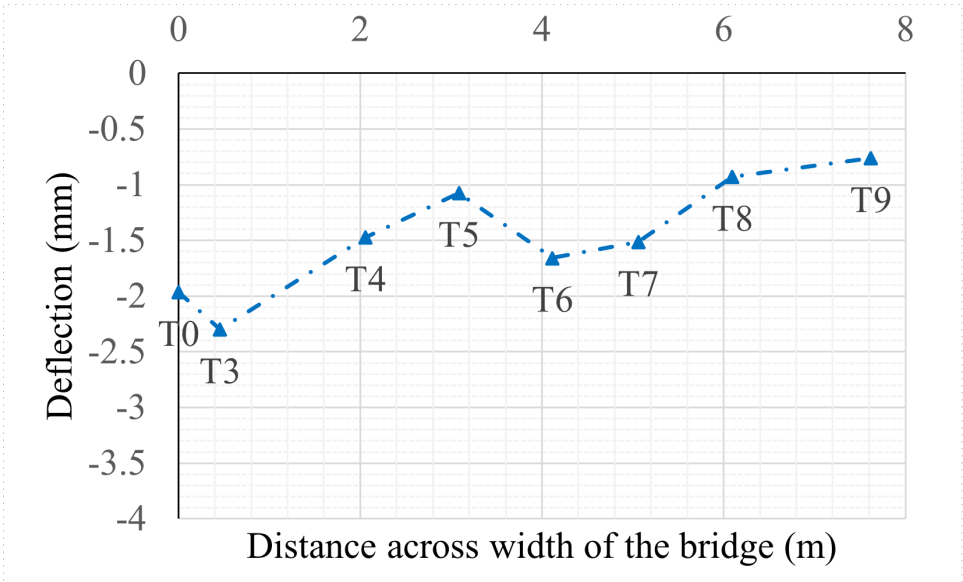

Figure 3-8: Deflection of the target across width of the bridge at midspan under fixed-location test 2

Even though two trucks were not used in the field, the deflections of targets under two trucks assuming symmetric behavior for the bridge are estimated and displayed in Figure 3-9.

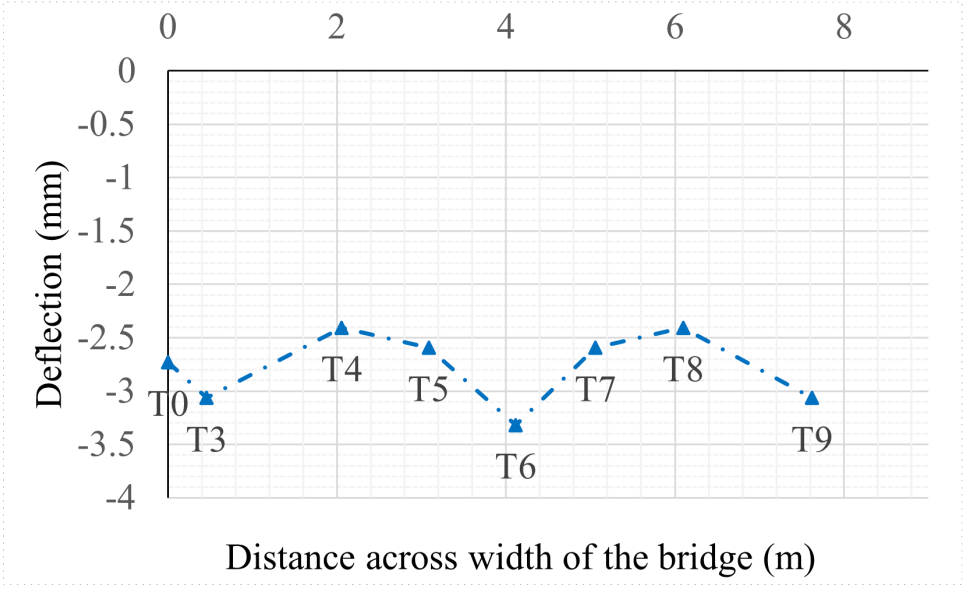

Figure 3-9: Assumed deflections across bridge cross-section under two trucks with tandem axel position over midspan

3.2.3.2 Experimental Distribution Factor (DFM)

The bridge slab is subdivided into seven longitudinal strips centered at the midspan targets that were tracked during load testing (targets 3, 4, 5, 6, 7, 8, and 9 in Figure 3-3). The distribution factors assigning the portion of the live load to each slab strip(g_Δ), can be calculated using equation (1 taken from [8], which is based on their relative stiffnesses.

$$g_\Delta = \frac{\Delta_i k_i}{\sum(\Delta_i k_i)} \quad (1)$$

Where, g_Δ is the live load distribution factor that is assigned to each slab strip takes, Δ_i is the deflection of midspan of each strip, and k_i is the vertical translation stiffness of each strip at the measurement point (midspan).

For the bridge in Case 1, all slab strips all have the same span, thickness, and material properties. Assuming that they also have a similar level of cracking that resulted from a similar loading history [9], then their relative stiffnesses can be related only using the width of each strip (w_i). Therefore, the distribution factor equation can be re-written as:

$$g_\Delta = \frac{\Delta_i w_i}{\sum(\Delta_i w_i)} \quad (2)$$

The slab strip widths differed for each strip as provided in Table 1. Therefore, to obtain the worst loading case, the strip distribution factors, g_{Δ}, were normalized by the strip width to obtain the worst fraction of a single truck load carried by a unit width of slab (DFM in Eq (3)).

$$DFM = \frac{\Delta_i}{\sum(\Delta_i w_i)} \tag{3}$$

Experimental DFM for each strip are summarized in Table 1 for the fixed-location test 2 with tandem axles at midspan and the projected two-truck loading scenario with two-truck loading with tandem axles at midspan. As can be seen in the table, the edge of the worst condition for single-truck loading occurs at bridge edge where a 1m strip carries about 18.9% of the truck load. For dual truck loading, the worst case occurs at the slab edge as well as along the centerline with about 13% of a single truck load carried by a 1m strip of slab.

Table 3-1: Calculations of experimental DFM for each strip under fixed-location loading with tandem axels at midspan and for single-lane loading and projected two-lane loading

Strip Number	Fixed-location test 2 with single-lane loaded			Fixed-location test 2 Projected to two-lane loading		
	$\Delta_i(\mathbf{mm})$	w_i(m)	*DFM (LL fraction/m)*	$\Delta_i(\mathbf{mm})$	w_i(m)	*DFM (LL fraction/m)*
1	2.300	1.32	0.189	3.064	1.32	0.121
2	1.474	1.34	0.121	2.406	1.34	0.095
3	1.075	1.06	0.088	2.592	1.06	0.102
4	1.658	1.04	0.136	3.316	1.04	0.131
5	1.516	1.04	0.124	2.592	1.04	0.102
6	0.9301	1.30	0.076	2.406	1.30	0.095
7	0.763	1.98	0.062	3.064	1.98	0.121

The equivalent slab width over which a single truck loading is carried is calculated as the inverse of the DFM values. Equivalent width values are compared with recommended values by AASHTO Standard Specification and AASHTO LRFD [6] in Figure 3-10. In this test, strips 1 and 4 under two-lane loading are the controlling strips since they have the highest distribution factor DFM, or conversely, the lowest equivalent width. The equivalent width estimated for these strips is approximately 4 m. This value is 15% higher than the width calculated using AASHTO LFR [10] method and 24% higher than the width calculated using the AASHTO LRFD method [6]. Both standard methods for estimating load distribution in this flat slab bridge conservative and could benefit from updating to reduce load posting outcomes for this type of bridge.

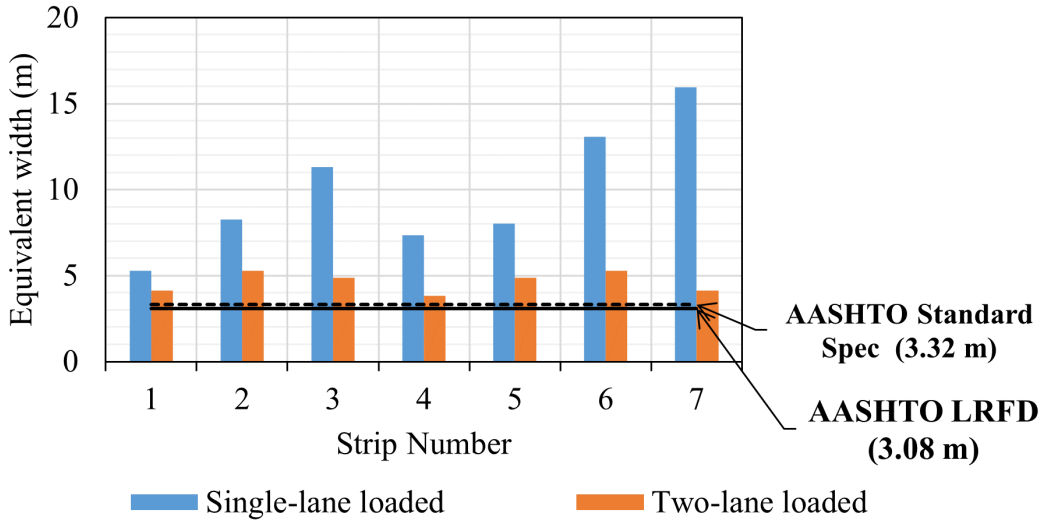

Figure 3-10: Comparison of estimated equivalent widths for each strip with AASHTO methods.

3.3 Case study 2: Multi girder steel bridge

3.3.1 Bridge description

The bridge considered in this case study is a steel multi-girder bridge located in Texas and built in 1934 (Figure 3-11). It carries two lanes of traffic for one direction of traffic, while an adjacent and separate bridge carries two lanes of traffic in the other direction. The bridge is on a main roadway with a high Annual Average Daily Traffic (AADT) count. The bridge has six spans with zero skew angle with total bridge length of 103.6 m (340 ft). The bridge consists of 3 simply supported spans, two anchor spans with cantilevers and one suspended span. Spans 1,2 and 3 have center to center span lengths of 15.85 m (52 ft), spans 4 and 6 are the anchor spans with center-to-center span length of 15.85 m (52 ft) and span 5 is a suspended span sitting on two 4.27m (14 ft) length cantilevers. The bridge has steel railings with 68.58 cm (27 in.) height. The bridge has a 20.32 cm (8 in.) concrete deck with and 5 cm (2 in.) of asphalt overlay. The bridge deck was measured to be 9 m (29.5 ft) wide with an approach roadway width of 8.53 m (28 ft). Per the NBI 2016, the bridge deck condition rating is 7 (good with some minor problems), the superstructure and substructure condition rating is 6 (Satisfactory with minor deterioration of structural elements). This study only focuses on suspended simply-supported span (span 5) since this span is the controlling span per load rating procedures. Girder properties and the distance between them are displayed in Figure 3-12.

It should be noted that the bridge was widened on the east side in 1967 by adding a steel channel. This girder which hereby is referred to as girder 6 (G6) is sitting on G5 and not a pier.

Conservatively, the contribution of this girder in estimation of Live Load Distribution Factors (LLDFs) is neglected.

Figure 3-11: image of bridge

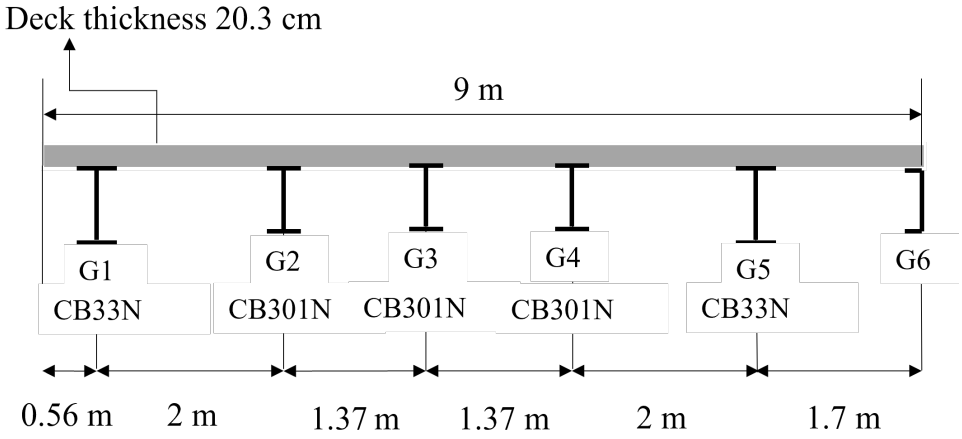

Figure 3-12: bridge suspended span section

3.3.2 Load testing procedures

The primary objective for load testing was to obtain data from which live load distribution among the steel girders could be determined. Deflection data were the primary data used in the analyses. The procedure of load testing with the CIV system for this bridge is very similar to the one used in the previous case study with this difference that this time the HCPTs are attached to steel girders at midspan of the controlling span (Figure 3-13). Two trucks were used in load testing of this bridge.

As mentioned before, the CIV software calibrated for bridge application has a measurement volume with distance to cameras between 12.2 m (40 ft) and 33.5 m (110 ft). In this case study,

due to restricted space around the bridge, the left camera optical axes was inclined to the bridge longitudinal axis. The cameras were placed approximately 16.76 m (55 ft) away from the first girder and 22.25 m (73 ft) away from the last girder (G6). Three targets were selected on the first girder to defining a user coordinate system that aligned with bridge main axes (Figure 14). Measured movements of the targets were provided with respect to this user-defined coordinate system. The field of view of the left camera, the selected targets in the CIV system, their numbers, and the coordinate system are shown in Figure 3-14.

Figure 3-13: attachment of HCPTs to the bridge steel girders.

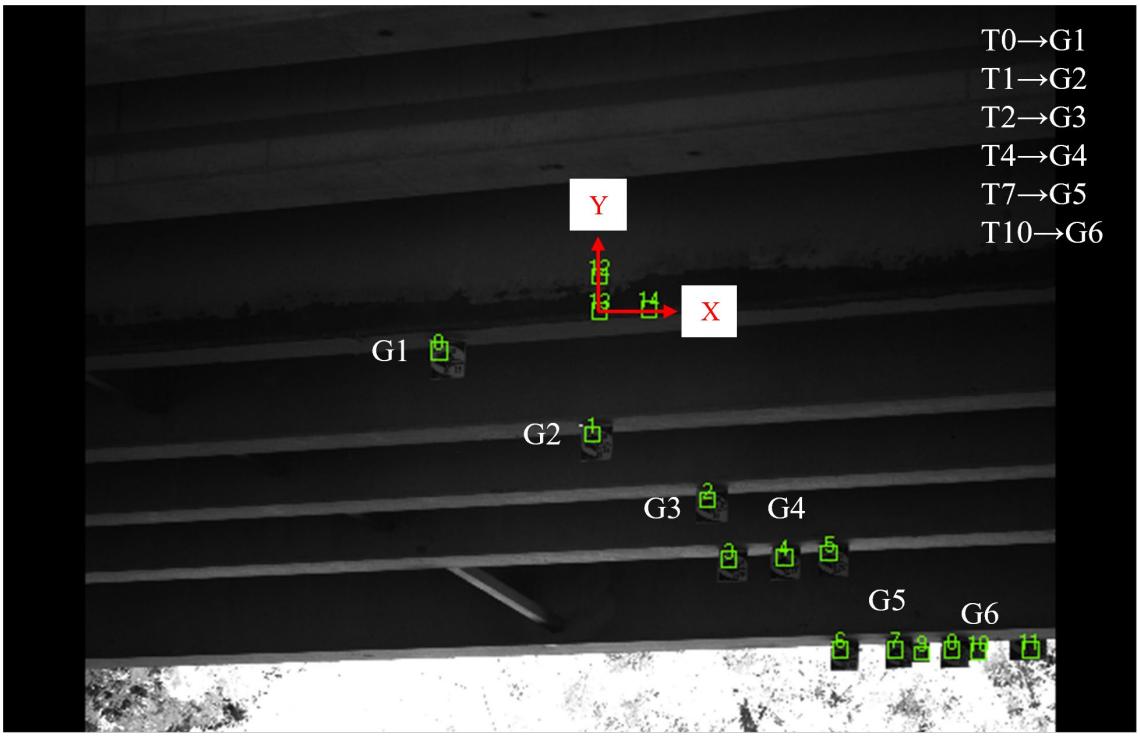

Figure 3-14: HCPTs selected in the CIV system and the defined new coordinate system

Two load testing paths were selected for this load test (Figure 3-15). Since the controlling girder for this span was G5, based on AASHTO load rating procedures, truck paths were selected to maximize loading on that girder. The first path placed a truck with the edge on its wheels on the outer edge on the lane above G5 as permitted in AASHTO MBE section 8. The other truck path placed the second truck centered across the width of the lane farther from girder G5.

The dump trucks used for testing had one front single axle and one tandem rear axle, as depicted in Figure 3-16. The weight of each truck was measured and they had approximately the same weight. The front axle of the trucks weighed about 53.38 kN (12,000 lbs), while the tandem axle weighed 151.23 kN (34,000 lbs).

For the single-truck loading test, the loaded truck was stopped in two positions along the path above G5, during which time deflection data were recorded. In the first position, (fixed location test 1) the front wheels were located at midspan along the path, while for the second position (fixed-location test 2), the rear tandem wheels were placed at midspan. For the double-truck loading test, both trucks were stopped with rear tandem wheels placed at midspan (fixed-location test 3). Similarly, to the previous case study, before each test, the three-dimensional location of targets was recorded with no traffic load on the bridge and used as the baseline locations from which deflections were calculated. For each fixed-location test, the truck was stopped for less than a minute at the desired location and the engine cut to minimize bridge vibrations. Images were recorded at three frames per second.

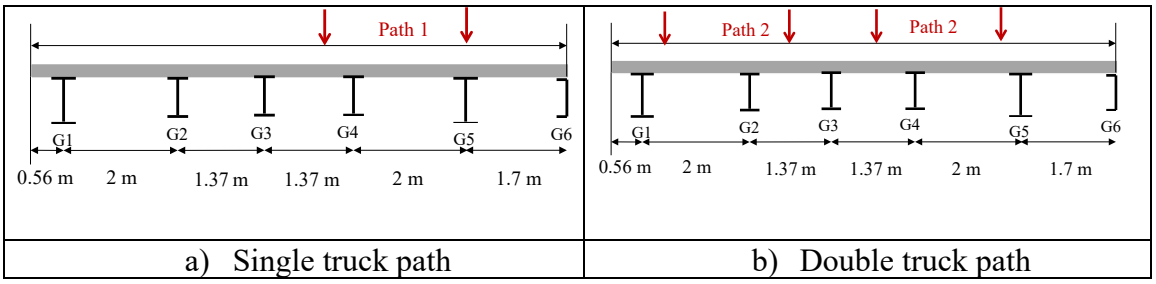

Figure 3-15: Bridge cross-section and truck path a) single truck path b) double truck path

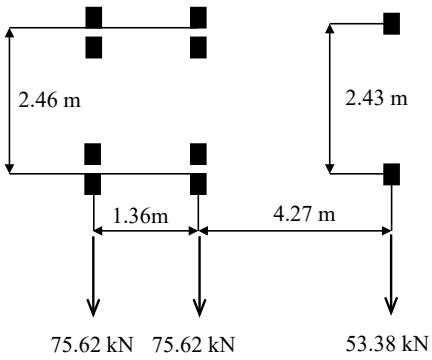

Figure 3-16: Trucks properties.

3.3.3 Load testing results

3.3.3.1 Deflection measurements

The history of the vertical deflections for fixed-location test 2 are presented in Figure 3-17. All the girders deflected under the load of single truck, which indicates that each contributed to carrying the truck load. Average deflections of G1, G2, G3, G4, G5 and G6 under the single-truck tandem axle test were 0.75 mm (0.029 in), 3.33 mm (0.13 in), 5.81 mm (0.22 in), 8.79 mm (0.35 in), 11.61 mm (0.46) and 13.67mm (0.54) respectively.

Figure 3-18 displays the mean deflection measurements of steel girders for all three fixed-location loads configurations. In Table 3-2, the mean deflections of the girders during the three load test configurations are summarized.

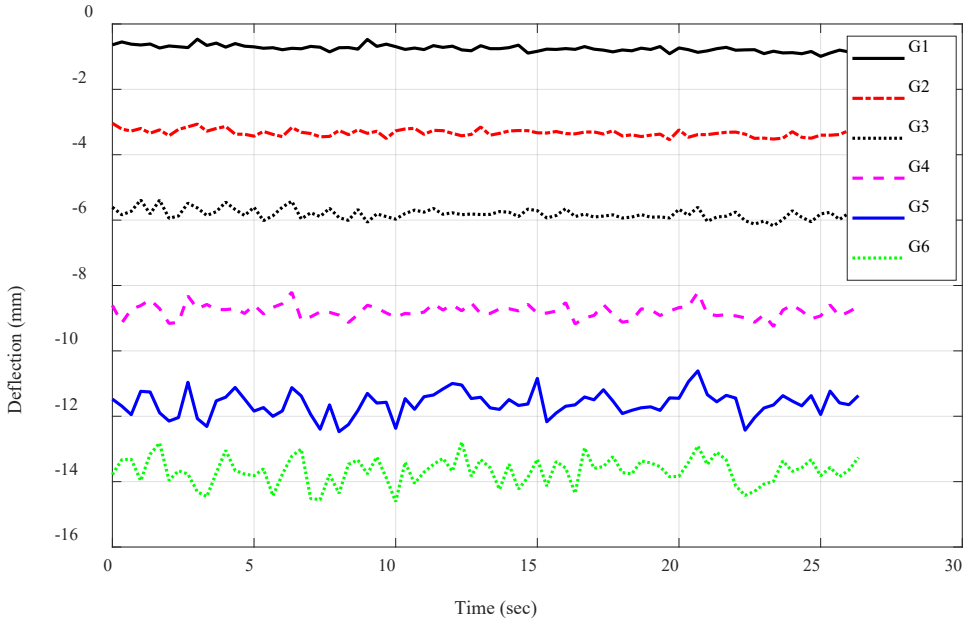

Figure 3-17: Vertical deflection histories of midspan targets during fixed-location test 2 (under tandem axle)

Figure 3-18: Deflection of the steel girders at midspan under fixe-location test 2

3.3.4 Experimental LLDFs

Live Load Distribution Factors (LLDFs) for bending moments were determined based on measurements from the load testing, AASHTO standard specification [11] and AASHTO LRFD bridge design specification [12]. LLDF for bending are the focus of this study as the moment capacity was the controlling capacity of this bridge (particularly for G5). The moment LLDF obtained by the load test were calculated as:

$$g_\Delta = m\frac{\Delta_i I_i}{\sum(\Delta_i I_i)} \qquad (4)$$

Where, m is the multiple presence factor per AASHTO LRFD, which is 1.2 for single-lane loading and 1.0 for two-lane loading, g_Δ is the live load distribution factor based on midspan deflections, Δ_i is the deflection of each girder, I_i is the composite section moment of inertia consisting of I-girder and the slab spanning half-way to adjacent girders. This choice of considering the composite section for the moment of inertia (I) is independent of whether composite actions is considered when calculating girder strength. This choice was made here as it provided an upper bound solution to the contribution of girder G5 as provided by the LLDF. Girder G5 has a larger slab width resting on it, which makes it moment of inertia, assuming slab composite action, larger proportionally to other girders, and therefore provides a larger LLDF for G5. LLDF of the girders for all the load tests are summarized in Table 3-2.

Table 3-2: Measured test deflections and corresponding girder LLDFs

Girder	G1	G2	G3	G4	G5
Fixed-location test 1 disp (mm)	0.083	2.029	3.995	6.195	8.722
Fixed-location test 1 LLDF	0.005	0.112	0.201	0.311	0.571

Girder	G1	G2	G3	G4	G5
Fixed-location test 2 disp (mm)	0.747	3.332	5.814	8.791	11.613
Fixed-location test 2 LLDF	0.0308	0.129	0.203	0.308	0.529
Fixed-location test 3 disp (mm)	12.019	13.015	12.812	12.794	12.185
Fixed-location test 3 LLDF	0.496	0.502	0.448	0.448	0.555

Figure 3-19 compares LLDF from load testing with those calculated using AASHTO standard specifications (LFR) and AASHTO LRFD (LRFR) values. As can be seen in Figure 18 and Figure 3-19, when one truck loading is applied, the farthest girder G1 deflects relatively little and as such resists a small fraction of the truck load. Despite both bridges in this study having approximately the same width, the farthest members resisted significantly different fractions of the single truck loading, with the farthest slab strip in the first case study resisting about 1/3 of the load resisted by the most heavily loaded strip, while girder G1 resisted less than 6% of the load on girder G5. This indicates that live load distribution should account for bridge system and the relative stiffness between girders and slab deck, which is not the case in LFR or LRFR load rating procedures.

For two truck loading, all five girders in the bridge resisted about the same fraction of about 50% of a truck loading. For the edge girder G1, a smaller LLDF was obtained than for the other edge girder G5. This may be attributed to the fact that G5 supports a larger overhang than G1.

From Figure 3-19, it can be seen that for all girders but G5, the AASHTO LRFD LLDF are only moderately more conservative than those obtained from load testing. Similarly, moderately more conservative values of LLDF are obtained from ASHTO LFR procedures compared with load testing results. Because of the widening of the bridge, the horizontal distance from the centerline of the exterior web of G5 to the interior edge of the curb (d_e) is 1.7m (5.57 ft), and therefore, the live LLDF is estimated as 0.76 based on AASHTO LRFD; which is about 27% higher than LLDF obtained by load testing. It is noted that load testing placed the truck closest to G5 at the edge of the lane as permitted in the AASHTO MBE, instead of 610mm from the edge of the curb, which is assumption for design. This discrepancy may have contributed to the relatively large difference in LLDF for G5. Using AASHTO standard specification equation for external girders, load sharing for G5 is calculated as 0.63 which is about 10% higher than LLDF obtained by load test. On the other hand, for G1, because of the short overhang, values recommended by the AASHTO standard specification is unconservative.

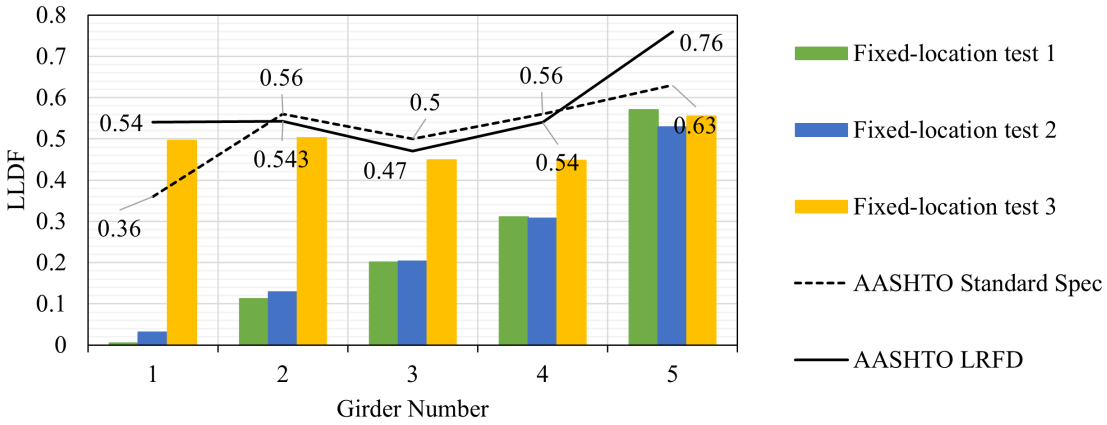

Figure 3-19: Live Load Distribution Factors for girders using load test deflection measurements, compared to LLDF estimated using AASHTO standard specifications and AASHTO LRFD

3.4 Summary and Conclusions

Load testing results demonstrate the potential of load rating improvement through load testing for concrete flat slab bridges and multi-girder steel bridges that are the most common types of bridges that are load posted without showing signs of structural distress in the state of Texas.

Formulas for calculating LLDF based on AASHTO standard specifications (LFR) do not take into account deck stiffness and span length, which makes this method less accurate and different than the LLDF obtained through load testing. For the flat slab bridge that was load tested, estimated equivalent widths based on load testing were 15 to 25% higher than those estimated by AASHTO standard specification (LFR) and the AASHTO LRFD procedures.. For the steel multi-girder bridge, the Live Load Distribution Factors (LLDF) obtained from load tests were generally less than 15% lower than the ones calculated based on LFR and LRFD procedure, with the LFR procedures showing unconservative results for one girder. Load testing results therefore indicate that LFR and LRFD procedures are moderately over-conservative for the bridges that were tested. Both procedures were more accurate (less conservative) for the steel girder bridge than the concrete slab bridge. Results therefore indicate that both bridges and particularly concrete slab bridges may benefit from improved load distribution formulations.

4 Value of Research

TxDOT has identified over two thousand deficient bridges requiring load posted, as listed in the National Bridge Inventory database[13]. TxDOT uses three categories for condition classification: (1) structurally deficient (SD), (2) functionally obsolete (FO), and (3) sub-standard for load only (SSLO). Structurally deficient bridges are those showing signs of deterioration and reduction in load capacity. Functionally obsolete bridges no longer fulfill their function, due to deficiencies such as roadway geometry and alignment issues. The SSLO classification introduced by TxDOT is for bridges that do not show signs of deterioration yet fail load rating checks and require load posting.

The most prevalent bridge types that are load-posted in Texas are: 1- Steel I-beam (803 bridges, 394 of them SSLO), Concrete flat slabs (388 bridges, 221 of them SSLO), and concrete slab and girder – pan formed (191 bridges, 106 of the SSLO). For these three bridge types there are therefore a total of 721 SSLO bridges that are load posted.

Based on the study presented in Chapter 3, Load testing of the two most prevalent SSLO bridge types can produce gains in load rating of up to 25%. Noting that typically SSLO bridges do not pass load rating by a small margin and particularly for heavier load from specialized hauling vehicles or emergency vehicles, it is postulated that up to 30% of SSLO bridges may be found to have adequate load capacity based on load testing results; and therefore can benefit directly form the product of this project (the CIV system).

Conservatively for this VOR analysis, it is assumed that only 10% of the 721 SSLO bridges, or 72 bridge, would see their load capacity deemed adequate after load testing; and therefore no longer require load posting or intervention. Again conservatively, the cost of remediating a bridge to increase its load capacity is at last $600,000 per bridge. On the other hand, as a result of this project, the CIV system allows TxDOT now to conduct load testing for a bridge in half a day and process the data to arrive at an adjusted load rating in only a few days, the cost of conducting load testing is relatively low should not exceed $30,000 per bridge, particularly when several bridge load tests are grouped and conducted in clusters. Off course not all bridges will benefit from load testing. About 30% of the SSLO bridges have load ratings that are within 10% of the required capacity and are the prime candidates for load testing. Therefore for each 3 load tests, one is expected to yield an outcome where no remedial action is required. The savings that can be derived from this project outcomes are conservatively $600,000-3x$30,000 = $510,000 per bridge and can total therefore 72x$510,000 = $36,720,000 only when it comes to cost of intervention.

This implementation project cost was $83,176 while the research project it utilizes 0-6950 had a cost of $419,432. The total research cost is therefore $502,608. Total cost savings from this research project are therefore anticipated to be over $36 million.

These cost savings can be realized gradually as load testing is conducted in the state. However given the speed and ease of using the CIV system, the necessary load tests can be conducted in about two years with investment in load testing personnel.

In addition, removing load posting on bridges would facilitate the transportation of good and people around the state, generating savings to the users that could easily add up to the intervention savings listed above. Such cost savings could be quantified using a network analysis regarding freight movement in the state, but is out of the scope of this study.

5 References

1. Ghannoum W. M., Diaz M., Rajae S., Banjade S., Chapagain B., Hogsett G., "CIV - Civil Infrastructure Vision© v1.0: Bridge Calibration User Manual and Validation Manual." Center for Transportation Research (CTR), FHWA/TX-21/0-6950-1, 2021, 85.
2. MBE AASHTO, "Manual for Bridge Evaluation, 3rd Edition," *American Association of State Highway and Transportation Officials, Washington, DC*, 2018.
3. Texas Department of Transportation, "Bridge Inspection Manual," Texas Department of Transportation (TXDOT)2020, 144.
4. Chapagain B., "Evaluating Bridge Behavior using Ultra-High Resolution Next Generation Digital Image Correlation (DIC) Applications in Bridge Inspection and Damage," San Antonio, TX: University of Texas at San Antonio, Master of Science, 2019, 170.
5. Banjade S., "Optimization and Accuracy Validation of Civil Infrastructure Vision (CIV) System for Large Scale Calibrations," San Antonio, Texas: University of Texas at San Antonio, Master of Science, 2021, 123.
6. AASHTO, "AASHTO LRFD Bridge Design Specifications, Eighth Edition," *American Association of State Highway and Transportation Officials, Washington*

DC 2017.
7. Sokoli Drit, Shekarchi William, Buenrostro Eliud, Ghannoum Wassim M %J Earthquakes, Structures, "Advancing behavioral understanding and damage evaluation of concrete members using high-resolution digital image correlation data," V. 7, No. 5, 2014, 609-26.
8. Fu Chung C, Elhelbawey Maged, Sahin MA, Schelling David R %J Journal of Structural Engineering, "Lateral distribution factor from bridge field testing," V. 122, No. 9, 1996, 1106-9.
9. Kwon Jinhan, Ghannoum Wassim M %J Engineering Structures, "Assessment of international standard provisions on stiffness of reinforced concrete moment frame and shear wall buildings," V. 128, 2016, 149-60.
10. Officials Transportation, "Standard specifications for highway bridges." Aashto, 2002.
11. AASHTO (2002). “Standard Specifications for Highway Bridges 17th Edition.” American Association of State Highway and Transportation Officials, Washington, DC. .
12. AASHTO, "AASHTO LRFD Bridge Design Specifications," *American Association of State Highway and Transportation Officials*, V. Eighth Edition, 2017.
13. Hueste M. B., Hurlebaus S., Mander J., Paal S., Terzioglu T., Stieglitz M., et al., "DEVELOPMENT OF A STRATEGY TO ADDRESS LOAD POSTED BRIDGES THROUGH REDUCTION IN UNCERTAINTY IN LOAD RATINGS —VOLUME 3: REFINED LOAD RATING RECOMMENDATIONS AND EXAMPLES." Texas A&M University, FHWA/TX-19/0-6955-R1-Vol3, 2019, 229.